ARTICLES
https://doi.org/10.1038/s41560-019-0374-6
nature energy

Co-electrolysis of CO_2 and glycerol as a pathway to carbon chemicals with improved technoeconomics due to low electricity consumption

Sumit Verma[1,2], Shawn Lu[1] and Paul J. A. Kenis[1,2*]

The renewable electricity-driven electroreduction of carbon dioxide (CO_2) offers an alternative pathway to producing carbon chemicals that are traditionally manufactured using fossil fuels. Typical CO_2 electroreduction approaches couple cathodic CO_2 reduction with the anodic oxygen evolution reaction (OER), resulting in approximately 90% of the electricity input being consumed by the OER. Here, we explore alternatives to the OER and show that the anodic electro-oxidation of glycerol (a byproduct of industrial biodiesel and soap production) can lower electricity consumption by up to 53%. This reduces the process's operating costs and carbon footprint, thus opening avenues for a carbon-neutral cradle-to-gate process even when driven by grid electricity (~13% renewables today), as well as economical production of the 12-electron products ethylene and ethanol. This study may thus serve as a framework for the design of CO_2 electroreduction processes with low electricity requirements, enhancing their CO_2 utilization potential and economic viability.

To limit excess anthropogenic carbon dioxide (CO_2) emissions (~4 GtC yr^{-1})[1] and achieve the 2 °C target set forth in the Paris Agreement on climate change[2], a portfolio of technologies, such as transitioning from fossil fuels to renewable energy (wind, solar, biofuels and so on), improving the energy efficiency of vehicles and buildings, and CO_2 capture and sequestration need to be implemented together[3]. However, for the majority of these solutions, the associated costs and impacts on economic growth are high, which contributes to slow global adoption[4,5]. In addition to mitigating CO_2 emissions, CO_2 can be utilized as a resource to produce carbon chemicals, such as formate/formic acid ($HCOO^-$/HCOOH), carbon monoxide (CO), methane (CH_4), methanol (CH_3OH), ethylene (C_2H_4) and ethanol (C_2H_5OH) via an electrochemical (that is, electroreduction) approach[6,7]. Such chemicals will be needed for a long time in the future but are currently manufactured using carbon-intensive fossil fuel methods (Fig. 1)[8–13]. The electroreduction of CO_2 to manufacture carbon chemicals could be a more sustainable alternative to such difficult-to-decarbonize methods.

Since the mid-1980s[14,15], numerous studies have focused on developing new catalysts, electrolytes and reactors for CO_2 electroreduction[16–21]. Recently, we evaluated the technoeconomic viability of CO_2 electroreduction using a high-level gross margin[22], and a modified US Department of Energy H2A model[23]. The results of the two analyses indicated that a significant lowering of the overall electricity consumption, and hence the cell potential, is necessary to improve the economics of CO_2 electroreduction. The current share of low carbon renewables in the US electricity grid is low (13%)[24] and projected not to exceed 30% by 2040 (Supplementary Table 1)[25]. Being able to drive CO_2 electroreduction using grid electricity (instead of pure renewables) and still be carbon neutral and/or negative from the cradle to the gate would be a holy grail scenario, as that would enable implementing the process into the existing infrastructure.

Here, we expand on the technoeconomic evaluation to investigate whether the electroreduction of CO_2 could become carbon neutral and/or negative from the cradle to the gate even with grid electricity. The evaluation suggests that such a scenario is possible if the CO_2 electroreduction cell potential is lowered. Most current CO_2 electroreduction approaches consist of the cathodic CO_2 reduction coupled to the anodic oxygen evolution reaction (OER). Thermodynamic analysis of these reactions shows that ~90% of the overall energy (hence, cell potential) requirements come from the OER. Thus, utilizing anode reactions with energy requirements lower than the OER could be a step change strategy for radically lowering the energy (hence, cell potential) requirements for CO_2 electroreduction. Here, we investigate such alternatives using a combined theoretical (thermodynamic) and experimental (electroanalytical) approach. Of the several options, the anodic oxidation of glycerol (a cheap byproduct of industrial biodiesel and soap production)[26,27], coupled to the cathodic reduction of CO_2 (that is, co-electrolysis of CO_2 and glycerol) seems particularly promising. The process lowers the CO_2 electroreduction cell potential by ~0.85 V, resulting in a reduction in the electricity consumption by up to 53%. In principle, this could drastically reduce the cradle-to-gate CO_2 emissions and improve the economics of CO_2 electroreduction.

Cradle-to-gate CO_2 emissions analysis

The overall CO_2 electroreduction process (and also the scope of the cradle-to-gate analysis) can be divided into four steps (Fig. 2), with the CO_2 emission for each step ($kgCO_2\,kg_{product}^{-1}$) denoted by CO_2 $emission_{(i)}$ (where $i = 1$, 2, 3 or 4). Note that in this analysis, we are not accounting for the CO_2 release during end use (that is, the full life cycle). For example, if C_2H_5OH (to be used as a fuel) is the major product, CO_2 is released when C_2H_5OH is oxidized, which is ignored in the analysis. Step 1 consists of sourcing the CO_2 feed—preferably from an industrial point source—and typically involves CO_2 capture and purification. The energy requirements for step 1 can be written in terms of a lumped parameter (that is, the electricity

[1]Department of Chemical and Biomolecular Engineering, University of Illinois at Urbana-Champaign, Urbana, IL, USA. [2]International Institute for Carbon Neutral Energy Research (WPI-I2CNER), Kyushu University, Fukuoka, Japan. *e-mail: kenis@illinois.edu

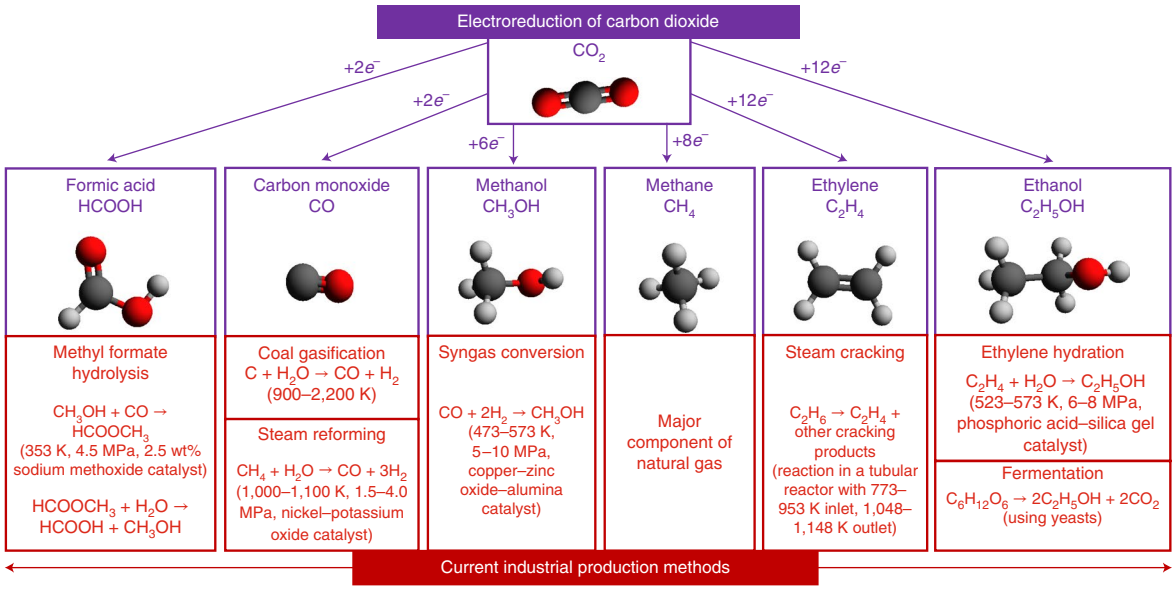

Fig. 1 | Overview of select CO_2 electroreduction products, along with the current industrial methods to manufacture these products. The current large-scale methods to manufacture HCOOH, CO, CH_3OH, CH_4, C_2H_4 and C_2H_5OH are primarily fossil fuel based and, in most scenarios, require high pressure and/or high temperature to drive the process. The electroreduction of CO_2 could be an alternative sustainable pathway to such fossil fuel-based manufacturing methods.

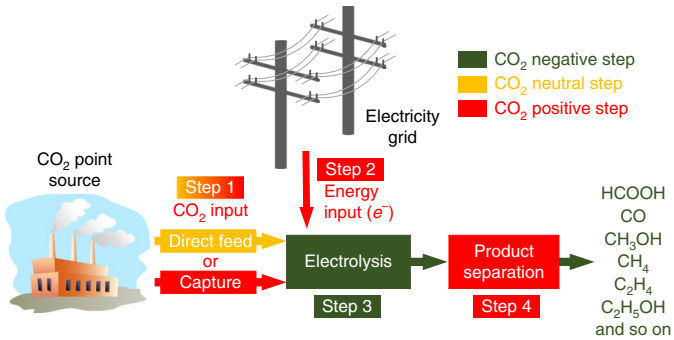

Fig. 2 | Scope of the cradle-to-gate CO_2 emissions analysis, and description of the steps involved in the industrial implementation of CO_2 electroreduction. Step 1 involves sourcing the CO_2 feed from point sources such as coal and natural gas power plants, cement plants, iron and steel plants, ethylene oxide production, ammonia, natural gas processing and so on. Step 2 involves the generation and delivery of electricity required to drive the electrolysis using the electricity grid. The use of renewables to drive the process of CO_2 electroreduction can be analysed as a special case of step 2. Step 3 involves the electroreduction of CO_2 to different carbon chemicals. Step 4 represents the separation process to obtain the purified product. The nature of CO_2 emission for each step is colour coded (green, CO_2 negative step (consumption); red, CO_2 positive step (emission); yellow, CO_2 neutral step).

equivalent, ε (in kWh $kgCO_2^{-1}$)[28], with the corresponding CO_2 emission$_{(1)}$ being estimated per equation (1):

$$CO_2\ \text{emission}_{(1)} = \text{GEF} \times \varepsilon \times \frac{n_{\text{carbon}} \times M_{CO_2}}{M} \quad (1)$$

where GEF is the grid (electricity generation) emission factor representing the energy-mix driving step 1 ($kgCO_2\,kWh^{-1}$), n_{carbon} is the number of carbon atoms in the CO_2 electroreduction product, M_{CO_2} is the molar mass of CO_2 ($g\,mol^{-1}$) and M is the molar mass of the CO_2 electroreduction product ($g\,mol^{-1}$). Note that GEF only considers emissions from the electricity generation (use phase) and not from the construction phase. Examples of CO_2 point sources include: coal or natural gas power plants; petroleum refineries; cement, iron and steel, C_2H_4, ethylene oxide, hydrogen (H_2) or C_2H_5OH (via fermentation) production plants; and ammonia or natural gas processing plants (Supplementary Table 2)[29]. Because the existing methods of C_2H_4, C_2H_5OH and H_2 production can, in principle, be replaced by CO_2 electroreduction and water electrolysis, the corresponding CO_2 sources are excluded from the discussion. In terms of purity and scale, the industrial data suggest that relatively pure CO_2 streams (>96%) are available from ethylene oxide production, or ammonia and natural gas processing, but at low production capacities (a combined output of <0.7% of the total US CO_2 emissions of ~5.6 $GtCO_2\,yr^{-1}$)[30]. Relatively larger sources of CO_2, such as cement, iron and steel plants (2.2% of total US CO_2 emissions combined) have a CO_2 purity of ~14–33%, whereas petroleum refineries (3.1% of total US CO_2 emissions) have a 3–100% CO_2 purity. The largest industrial sources of CO_2 (that is, coal and natural gas power plants) have a purity of 10–15% and 3–5%, respectively.

For the cradle-to-gate CO_2 emissions calculations in this work, we assume a base-case, best-case and worst-case scenario of utilizing the CO_2 captured from an iron and steel plant (energy required = 0.76 GJ tCO_2^{-1}; $\varepsilon = 0.211$ kWh $kgCO_2^{-1}$)[31], an ethylene oxide production, ammonia or natural gas processing plant (almost pure CO_2; hence, $\varepsilon = 0$) and a natural gas power plant ($\varepsilon = 0.297$ kWh $kgCO_2^{-1}$)[28], respectively. Another version of the best-case scenario would be to utilize flue gas directly[32]. However, further research needs to be performed to determine the effect of flue gas impurities (SO_x, NO_x and so on) on CO_2 electroreduction to evaluate such pathways.

Step 2 of the CO_2 electroreduction process consists of the generation, delivery and consumption of electricity to drive the reaction. Using Faraday's law of electrolysis, CO_2 emission$_{(2)}$ can be written as follows:

$$CO_2\ \text{emission}_{(2)} = \text{GEF} \times \frac{F \times z \times V_{\text{operating}}}{3,600 \times M} \quad (2)$$

where F is the Faraday constant (96,485 C mol^{-1}), z is the number of electrons exchanged to form the CO_2 electroreduction product and $V_{\text{operating}}$ is the operating cell potential (V). GEF for the current US electricity grid (13% renewables; 2014 data) is ~0.51 $kgCO_2$ kWh^{-1} (Supplementary Table 1)[24]. Such a scenario can be considered the worst case as well as the base case for our analysis, implementing the CO_2 electroreduction process into the existing infrastructure. The best case for step 2 would be the utilization of future grid electricity projections (2040; 28% renewables per the US Energy Information Administration[25]). Assuming the emission factor for individual electricity sources remains invariant over time, the GEF for 2040 can be estimated by extrapolating the 2014 data, resulting in a value of ~0.35 $kgCO_2$ kWh^{-1} (Supplementary Table 1)[25].

Step 3 of the process is the CO_2-consuming electroreduction step. Its emissions are defined as follows:

$$CO_2\ \text{emission}_{(3)} = -\frac{n_{\text{carbon}} \times M_{CO_2}}{M} \quad (3)$$

Step 4 involves separation of the products. Figure 3a visualizes a simple scenario of separating one feed stream (stream 1) with two types of components (product and carrier) into a relatively pure product (stream 2) and a waste (stream 3), for which the energy demand and CO_2 emission$_{(4)}$ can be calculated based on the minimum work of separation (W_{min} (in kJ $mol_{\text{product}}^{-1}$)) in combination with the empirical second-law efficiency values (from ref. [33]) for different separation processes (equations (4) and (5)), as described earlier by House and coworkers[33]:

$$W_{\text{min}} = \frac{-RT}{1,000 \times N_{\text{product}}} \left(N_1 \sum_{k=\text{product, carrier}} x \ln \gamma_{1,k} x_{1,k} - N_2 \sum_{k=\text{product, carrier}} x_{2,k} \ln x_{2,k} - N_3 \sum_{k=\text{product, carrier}} x_{3,k} \ln x_{3,k} \right) \quad (4)$$

$$CO_2\ \text{emission}_{(4)} = \text{GEF} \times \frac{W_{\text{min}}}{0.036 \times M \times \eta_{\text{2nd law}}} \quad (5)$$

where R is the universal gas constant (8.314 J mol^{-1} K^{-1}), T is the temperature (298 K), N_j (where $j = 1$, 2 or 3) is the total number of moles in stream j, $x_{j,k}$ is the mole fraction of component k in stream j, $\gamma_{1,k}$ is the activity coefficient of component k in stream 1 (streams 2 and 3 are assumed to be relatively pure; hence, $\gamma = 1$ for the pure component), N_{product} is the number of moles of the recovered product, and $\eta_{\text{2nd law}}$ is the second-law thermodynamic efficiency for the separation process (%). The W_{min} values can further be used to identify the optimum mole fraction of the desired product in the electrolyser product stream ($x_{1,\text{product}}$), molar product purity ($x_{2,\text{product}}$) and product recovery (R_{product}). The graphs in Fig. 3b,c show the W_{min} requirements for separating a mixture of gaseous CO_2 electroreduction products and CO_2 carrier (assuming the gases behave ideally; $\gamma = 1$). Of the three separation parameters, W_{min} is the most sensitive towards $x_{1,\text{product}}$. A near-exponential drop in W_{min} is seen as a function of $x_{1,\text{product}}$ up to a value of approximately 0.2 (Fig. 3b). In contrast, the variation in W_{min} with $x_{2,\text{product}}$ and R_{product} is fairly modest, especially under industrially applicable ranges of $x_{2,\text{product}}$ and $R_{\text{product}} > 0.8$ (Fig. 3b,c)[33]. However, note that $\eta_{\text{2nd law}}$ also depends on the concentration in addition to the concentration factor, exact balance of the plant design, and degree of heat integration in the whole plant. These dependencies are not captured in the analysis here. Learning from the trends in W_{min}, and also to make our analysis industrially applicable as well as practically feasible (as shown by the process simulation and experimental data from the literature summarized in the supplementary information of ref. [33]), we assume $x_{1,\text{product}}$, $x_{2,\text{product}}$ and R_{product} values of 0.2, 0.99 and 0.9, respectively, for separating both the gaseous and liquid products. Also, note that for the electroreduction of CO_2, an $x_{1,\text{product}}$ value of 0.2 can be experimentally achieved by simply tuning (lowering) the flow rate of the carrier stream (that is, CO_2 for gas products) as shown in Supplementary Fig. 1. W_{min} requirements for separating the products of CO_2 electroreduction from the appropriate carrier streams are listed in Table 1, assuming $\gamma = 0.72$, 1.58, 3.74 and 0.90 for HCOOH, CH_3OH, C_2H_5OH and electrolyte (assuming 2.0 M KOH), respectively[34,35]. The HCOOH–electrolyte, alcohol (CH_3OH or C_2H_5OH)–electrolyte and gas product (CO, CH_4 or C_2H_4)–CO_2 mixtures can be assumed to be separated via liquid–liquid extraction, distillation and pressure swing adsorption, respectively. Using the $\eta_{\text{2nd law}}$ values of the different separation processes (Table 1)[33,36,37], the theoretical W_{min} values can be converted to the actual energy requirement using equation (5). Note that in the cradle-to-gate CO_2 emissions calculation described above, the emissions associated with the mining and usage of precious metal catalysts were ignored because a back-of-the-envelope calculation suggests that the rate of CO_2 emission associated with the use of platinum group metals (CO_2 emission factor = 51.2 tCO_2 kg_{metal}^{-1}; ref. [38]) for a typical industrial-scale electrolyser (catalyst loading = 0.5 mg cm^{-2} for both anode and cathode; catalyst use life = 10,000 h)[22] is just 0.051 $kgCO_2$ m^{-2} h^{-1}. To better gauge the significance of this CO_2 footprint, we can look at the case of converting CO_2 to CO at an industrially relevant current density of 200 mA cm^{-2} (CO production rate = 1.05 kgCO m^{-2} h^{-1}; CO_2 consumption rate = 1.65 $kgCO_2$ m^{-2} h^{-1}). The rate of CO_2 emissions due to the utilization of precious metal catalysts turns out to be <3% of the CO_2 consumption rate, indicating the emissions to be insignificant.

For the CO_2 electroreduction process to be carbon neutral and/or negative from the cradle to the gate, cumulative CO_2 emissions during steps 1–4 should be equal to or less than zero, resulting in an expression for the maximum operating cell potential ($V_{\text{max }(CO_2\ \text{emission})}$ (in V); equation (6)). Under different operating conditions, the operating cell potential ($V_{\text{operating}}$ (in V)) has to be equal to or less than $V_{\text{max }(CO_2\ \text{emission})}$ to realize a carbon neutral and/or negative process from the cradle to the gate. From a thermodynamic perspective, the $V_{\text{operating}}$ and $V_{\text{max }(CO_2\ \text{emission})}$

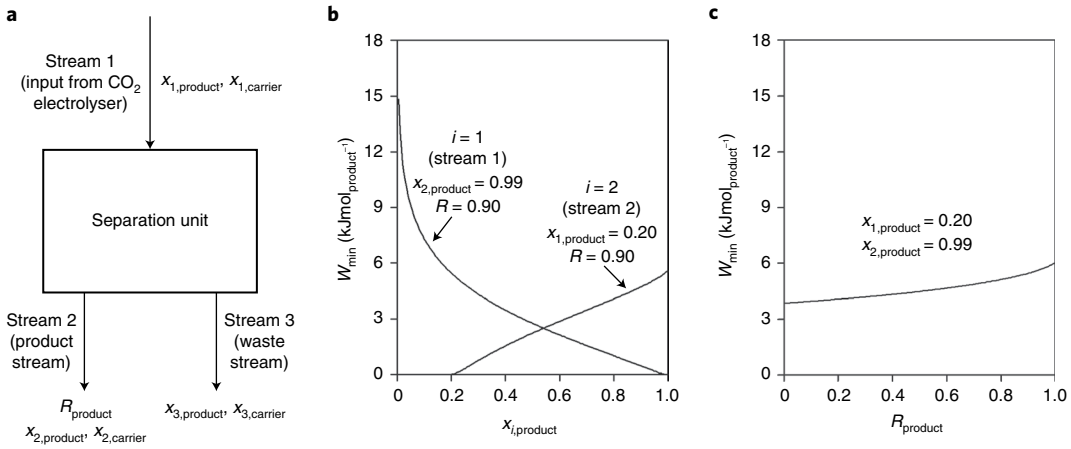

Fig. 3 | Optimizing separation parameters for the purification of CO_2 electroreduction products. a, Block flow diagram depicting the separation unit. The output stream of the CO_2 electrolyser is fed directly to the separation unit as stream 1. Stream 1 is assumed to be a binary mixture of the CO_2 electroreduction product and the carrier (that is, unreacted CO_2 for the gaseous products, and electrolyte (for example, 2.0 M KOH) for the liquid products). The input stream is separated into product stream 2 (product purity in mole fraction = $x_{2,product}$ and recovery = $R_{product}$) and waste stream 3. **b**,**c**, Variation in W_{min} required to separate stream 1 into streams 2 and 3, as a function of the product mole fraction in input stream 1 ($x_{1,product}$), as well as product purity ($x_{2,product}$) (**b**), and as a function of $R_{product}$ (**c**). Streams 1, 2 and 3 are assumed to be ideal gases with an activity coefficient (γ) of 1 for the calculations.

Table 1 | Maximum operating cell potential ($V_{max\ (CO_2\ emission)}$ and $V_{max\ (gross\ margin)}$) that can be utilized to drive the electroreduction of CO_2 in a carbon neutral/negative (from cradle-to-gate) and economically viable manner, respectively

Product	M (g mol^{-1})	z	n_{carbon}	Carrier stream	W_{min} (kJ mol$_{product}^{-1}$)	Separation method	$\eta_{2nd\ law}$ (%)	ε (kWh kg CO_2^{-1})	$V_{max\ (CO_2\ emission)}$ (V)		$V_{max\ (gross\ margin)}$ (V)[22]			$\lvert E^0_{cell}\rvert$ (V)[37]
									GEF (kgCO_2 kWh^{-1})		C_E (US$ kWh^{-1})			
									0.51	0.35	0.04	0.06	0.12	
HCOOH	46.02	2	1	Electrolyte (2.0 M KOH)	7.52	Liquid–liquid extraction	25	0.297	1.27	2.04[a]	16.74[b]	11.16[b]	5.58[b]	1.48
								0.211	1.35	2.12[a]				
								0	1.53[a]	2.30[a]				
CO	28.01	2	1	CO_2	5.45	Pressure swing adsorption	17	0.297	0.70	1.17	10.84[b]	7.23[b]	3.61[b]	1.34
								0.211	0.75	1.22				
								0	0.86	1.33				
CH_3OH	32.04	6	1	Electrolyte (2.0 M KOH)	5.35	Distillation	13	0.297	0.26	0.44	1.48[b]	0.99	0.49	1.21
								0.211	0.28	0.46				
								0	0.32	0.50				
CH_4	16.04	8	1	CO_2	5.45	Pressure swing adsorption	17	0.297	0.08	0.15	0.26	0.17	0.09	1.06
								0.211	0.09	0.16				
								0	0.11	0.17				
C_2H_4	28.05	12	2	CO_2	5.45	Pressure swing adsorption	17	0.297	0.26	0.42	1.81[b]	1.21[b]	0.60	1.17
								0.211	0.28	0.43				
								0	0.31	0.47				
C_2H_5OH	46.07	12	2	Electrolyte (2.0 M KOH)	2.98	Distillation	9	0.297	0.45	0.70	1.79[b]	1.19[b]	0.60	1.15
								0.211	0.47	0.73				
								0	0.53	0.79				

The $V_{max\ (CO_2\ emission)}$ values were obtained using equation (6). C_E is the electricity price. For the manufacture of a particular CO_2 electroreduction product in a carbon-neutral manner from the cradle to the gate, the required criterion is: $\lvert E^0_{cell}\rvert < V_{max\ (CO_2\ emission)}$. The $\lvert E^0_{cell}\rvert$ values are reported under standard conditions (1 atm and 298 K), assuming the electroreduction of CO_2 as the cathode reaction, and O_2 evolution ($E^0 = -1.23$ V versus RHE) as the anode reaction. $V_{max\ (gross\ margin)}$ values were obtained from ref. [22]. For the manufacture of a particular CO_2 electroreduction product in an economically viable manner, the required criterion is: $\lvert E^0_{cell}\rvert < V_{max\ (gross\ margin)}$. [a]Carbon-negative conditions from the cradle to the gate. [b]Economically viable conditions.

values will also have a lower bound, as determined by the standard thermodynamic cell potential ($\lvert E^0_{cell}\rvert$ (in V)), representing the theoretical minimum energy requirement. This results in an inequality expression (equation (7)) that needs to be satisfied at all times for a particular process to become carbon neutral and/or negative from the cradle to the gate. Note, that over the full life cycle (that is, including the CO_2 electroreduction product use), the process will be carbon negative only if the carbon is

Table 2 | Theoretical $\Delta G^0_{reaction}$ and $|E^0_{cell}|$ for the cathodic electroreduction of CO_2 to CO and C_2H_4, coupled to anodic O_2 evolution, or glycerol, glucose and CH_4 electro-oxidation

Cathode reaction	Possible anode reactions	Possible overall reactions	$\Delta G^0_{reaction}$ (kJ mol^{-1})	$\lvert E^0_{cell}\rvert$ (V)
$CO_2 \rightarrow CO$	Water → oxygen $2OH^- \rightarrow H_2O + 0.5O_2 + 2e^-$	$CO_2 \rightarrow CO + 0.5O_2$	257.20	1.33
	Glycerol → glyceraldehyde $C_3H_8O_3 + 2OH^- \rightarrow C_3H_6O_3 + 2H_2O + 2e^-$	$CO_2 + C_3H_8O_3 \rightarrow CO + C_3H_6O_3 + H_2O$	97.48	0.51
	Glycerol → lactic acid $C_3H_8O_3 + 2OH^- \rightarrow C_3H_6O_3 + 2H_2O + 2e^-$	$CO_2 + C_3H_8O_3 \rightarrow CO + C_3H_6O_3 + H_2O$	68.08	0.35
$CO_2 + H_2O + 2e^- \rightarrow CO + 2OH^-$	Glycerol → HCOOH $C_3H_8O_3 + 8OH^- \rightarrow 3HCOOH + 5H_2O + 8e^-$	$CO_2 + 0.25C_3H_8O_3 \rightarrow CO + 0.75HCOOH + 0.25H_2O$	46.53	0.24
	Glucose → gluconic acid $C_6H_{12}O_6 + 2OH^- \rightarrow C_6H_{12}O_7 + H_2O + 2e^-$	$CO_2 + C_6H_{12}O_6 \rightarrow CO + C_6H_{12}O_7$	6.20	0.03
	$CH_4 \rightarrow CH_3OH$ $CH_4 + 2OH^- \rightarrow CH_3OH + H_2O + 2e^-$	$CO_2 + CH_4 \rightarrow CO + CH_3OH$	141.10	0.73
	$CH_4 \rightarrow CO$ $CH_4 + 6OH^- \rightarrow 5H_2O + CO + 6e^-$	$0.75CO_2 + 0.25CH_4 \rightarrow CO + 0.5H_2O$	52.68	0.36
$CO_2 \rightarrow C_2H_4$	Water → oxygen $2OH^- \rightarrow H_2O + 0.5O_2 + 2e^-$	$2CO_2 + 2H_2O \rightarrow C_2H_4 + 3O_2$	1,331.40	1.15
	Glycerol → glyceraldehyde $C_3H_8O_3 + 2OH^- \rightarrow C_3H_6O_3 + 2H_2O + 2e^-$	$2CO_2 + 6C_3H_8O_3 \rightarrow C_2H_4 + 6C_3H_6O_3 + 4H_2O$	373.08	0.32
	Glycerol → lactic acid $C_3H_8O_3 + 2OH^- \rightarrow C_3H_6O_3 + 2H_2O + 2e^-$	$2CO_2 + 6C_3H_8O_3 \rightarrow C_2H_4 + 6C_3H_6O_3 + 4H_2O$	196.68	0.17
$2CO_2 + 8H_2O + 12e^- \rightarrow C_2H_4 + 12OH^-$	Glycerol → HCOOH $C_3H_8O_3 + 8OH^- \rightarrow 3HCOOH + 5H_2O + 8e^-$	$2CO_2 + 1.5C_3H_8O_3 + 0.5H_2O \rightarrow C_2H_4 + 4.5HCOOH$	67.35	0.06
	Glucose → gluconic acid $C_6H_{12}O_6 + 2OH^- \rightarrow C_6H_{12}O_7 + H_2O + 2e^-$	$2CO_2 + 6C_6H_{12}O_6 + 2H_2O \rightarrow C_2H_4 + 6C_6H_{12}O_7$	−174.60	0.15
	$CH_4 \rightarrow CH_3OH$ $CH_4 + 2OH^- \rightarrow CH_3OH + H_2O + 2e^-$	$2CO_2 + 6CH_4 + 2H_2O \rightarrow C_2H_4 + 6CH_3OH$	634.80	0.55
	$CH_4 \rightarrow CO$ $CH_4 + 6OH^- \rightarrow 5H_2O + CO + 6e^-$	$2CO_2 + 2CH_4 \rightarrow C_2H_4 + 2CO + 2H_2O$	209.60	0.18

$\Delta G^0_{reaction} = \sum \nu_{product} \times \Delta G^0_{f\,product} - \sum \nu_{reactant} \times \Delta G^0_{f\,reactant}$, where ν is the stoichiometric coefficient and ΔG_f^0 is the Gibbs free energy of formation (see Supplementary Table 3 for ΔG_f^0 values). $|E^0_{cell}| = |-\Delta G^0/z \times F|$, where z is the number of electrons transferred. All thermodynamic properties are reported under standard conditions (1 bar and 298 K). Note that the 10–20 mV difference in the $|E^0_{cell}|$ values between Tables 1 and 2, for the case of CO_2 electroreduction at the cathode and O_2 evolution at the anode, is due to the minor differences in the electrochemistry and thermochemistry data used to estimate $|E^0_{cell}|$ in Tables 1 and 2, respectively.

permanently stored in the product. However, is more likely that the carbon will be released again at the end of life, leading to a carbon-positive life cycle that can become carbon neutral at best.

$$V_{\max\,(CO_2\ \text{emission})} = \frac{3{,}600}{F \times z} \times \left[\left(\frac{1}{\text{GEF}} - \varepsilon \right) \times n_{carbon} \times M_{CO_2} - \frac{W_{min}}{0.036 \times_{2nd\ law}} \right] \quad (6)$$

$$|E^0_{cell}| \leq V_{operating} \leq V_{\max\,(CO_2\ \text{emission})} \quad (7)$$

Table 1 shows the calculated $V_{\max\,(CO_2\ \text{emission})}$ values (per equation (6)) for several CO_2 electroreduction products under different operating conditions. For a first-order estimate, the $|E^0_{cell}|$ values in Table 1 correspond to a typical CO_2 electroreduction process (that is, cathodic CO_2 electroreduction coupled to the anodic OER[39]). A comparison of the $V_{\max\,(CO_2\ \text{emission})}$ and theoretical $|E^0_{cell}|$ values indicates HCOOH to be the only product for which the inequality expression for a carbon-neutral and/or -negative cradle-to-gate process (equation (7)) is satisfied (that is, HCOOH in principle can be produced in a carbon-neutral and/or -negative manner from the cradle to the gate using grid electricity, albeit in special cases; that is, for the 2040 US grid scenario (28% renewables) or with pure CO_2 streams/direct flue gas ($\varepsilon = 0$)). For all of the other products, further reductions in the GEF (~0.31, 0.14, 0.06, 0.14 and 0.22 for CO, CH_3OH, CH_4, C_2H_4 and C_2H_5OH, respectively) will be required to achieve carbon neutrality from the cradle to the gate. Another interesting design strategy to satisfy the $V_{\max\,(CO_2\ \text{emission})}$ criterion (equation (7)) could be to utilize oxidation reactions at the anode other than the OER, leading to lower $|E^0_{cell}|$, as shown below. Such process design strategies could also improve the economic prospects of producing high-volume C_2H_4 and C_2H_5OH, which were initially deemed to be economically unfavourable (Table 1), per the gross margin model[22].

Identifying alternatives to the OER at the anode

A Gibbs free energy analysis of the conventional CO_2 electroreduction process indicates that the OER is significantly uphill (energetically) compared with CO_2 reduction. For example, consider the electroreduction of CO_2 to CO (equations (8)–(10)). Utilizing Hess's law to calculate the standard Gibbs free energy of the reaction ($\Delta G^0_{reaction}$ (in kJ mol^{-1})), as well as the energetics of the individual steps, we find that 92.2% of the overall energy is required to drive the OER at the anode. Hence, the design of alternative CO_2 electroreduction processes with anode reactions

other than the OER that can significantly lower the overall energy requirements (hence, $|E^0_{cell}|$) might lead to thermodynamically superior system designs.

$$CO_2 + H_2 \rightarrow CO + H_2O \quad (\Delta G^0_{reaction} = 20.10\ kJ\ mol^{-1};\ 7.8\%\ of\ total\ energy) \tag{8}$$

$$H_2O \rightarrow H_2 + 0.5O_2 \quad (\Delta G^0_{reaction} = 237.10\ kJ\ mol^{-1};\ 92.2\%\ of\ total\ energy) \tag{9}$$

$$Overall: CO_2 \rightarrow CO + 0.5O_2 \quad (\Delta G^0_{reaction} = 257.20\ kJ\ mol^{-1}) \tag{10}$$

The selection of the anode feed and the associated reactions to replace the OER can be guided by a simple set of process design rules: the production method (is the process energy intensive, resulting in additional CO_2 emissions?); the cost (is the anode feed a waste or an expensive chemical?); and the scale (can the anode reaction match the scale of CO_2-based commodity and intermediate chemicals production?). A few efforts in the CO_2 electroreduction literature have reported utilizing anode reactions other than the OER, but the reactions used do not satisfy the aforementioned design rules. For example, the electro-oxidation of C_2H_5OH to acetate at the anode has been used to lower the onset cell potential for CO_2 electroreduction from −2.31 to −1.26 V[40]. Similarly, the electro-oxidation of benzylic and aliphatic alcohols, such as 4-methoxybenzyl alcohol, 1-phenylethanol, C_2H_5OH and isopropanol, at the anode was used to replace the OER[41]. While such efforts are interesting, the oxidation of the reported alcohols may not be the best path forward. C_2H_5OH and isopropanol can, in principle, be obtained by CO_2 electroreduction[17–19]. Hence, oxidizing such alcohols at the anode would be equivalent to moving back and forth in a thermodynamic cycle. Meanwhile, 4-methoxybenzyl alcohol and 1-phenylethanol are fine chemicals for which there is not a demand at the scale of commodity and intermediate chemicals.

The electro-oxidation of high-volume building block chemicals such as glycerol (a cheap byproduct of biodiesel and soap manufacturing at industrial scales with 80% purity costs of about US$0.24 kg^{-1})[26,27,42], biomass-derived glucose, or even CH_4 (large natural gas reserves, otherwise flared-off gas at oil fields)[43], could satisfy the process design rules for the suitable anode reactions outlined earlier. Table 2 and Supplementary Table 4 show the calculated $\Delta G^0_{reaction}$ and $|E^0_{cell}|$ values for select combinations of CO_2 electroreduction with glycerol, glucose and CH_4 electro-oxidation. The results suggest that a significant lowering of $|E^0_{cell}|$, and hence electricity requirements, can be realized by moving away from the anodic OER. Several of the proposed processes also satisfy the $V_{max\ (CO_2\ emission)}$ criterion from Table 1, assuming that the anode feed is a waste product (that is, waste glycerol from biodiesel production or CH_4 from otherwise flared-off gas) with no extra CO_2 emissions[44], and the energy (also the associated CO_2 emissions) required to separate the anode product results in minimal changes in the $V_{max\ (CO_2\ emission)}$ values. One can validate this assumption by calculating the energy required to purify the anode products (for example, HCOOH, as observed in this work) using a process with minimum work requirement and CO_2 intensity for separation similar to that when produced on the cathode (W_{min} = 7.52 kJ mol$_{product}^{-1}$; $\eta_{2nd\ law}$ = 25%). In such scenarios, the $V_{max\ (CO_2\ emission)}$ values reduce by a maximum of 10%, indicating that the energy requirement for separation is not the most CO_2-intensive step, and comparisons with the $V_{max\ (CO_2\ emission)}$ values still hold. However, hypothetically, if the anode products were alcohols that would require a less efficient distillation process ($\eta_{2nd\ law}$ = 9–13%), the changes in $V_{max\ (CO_2\ emission)}$ would be 2–3 times higher. Also, the reader must note that emission credits may also be available for the anode product, which can further reduce the cradle-to-gate CO_2 footprint of the overall process. With alternate anode reactions, the electroreduction of CO_2 to CH_3OH, C_2H_4 and C_2H_5OH looks cost competitive as well (Table 2 and Supplementary Table 4), with more processes now starting to satisfy the $V_{max\ (gross\ margin)}$ requirements—processes that were initially unattainable with the OER at the anode (Table 1). Again, this reasoning is valid only under the assumption that either the anode feed is a cheap waste stream, or the cost of the anode feed and subsequent product separation is offset by the market value of the anode

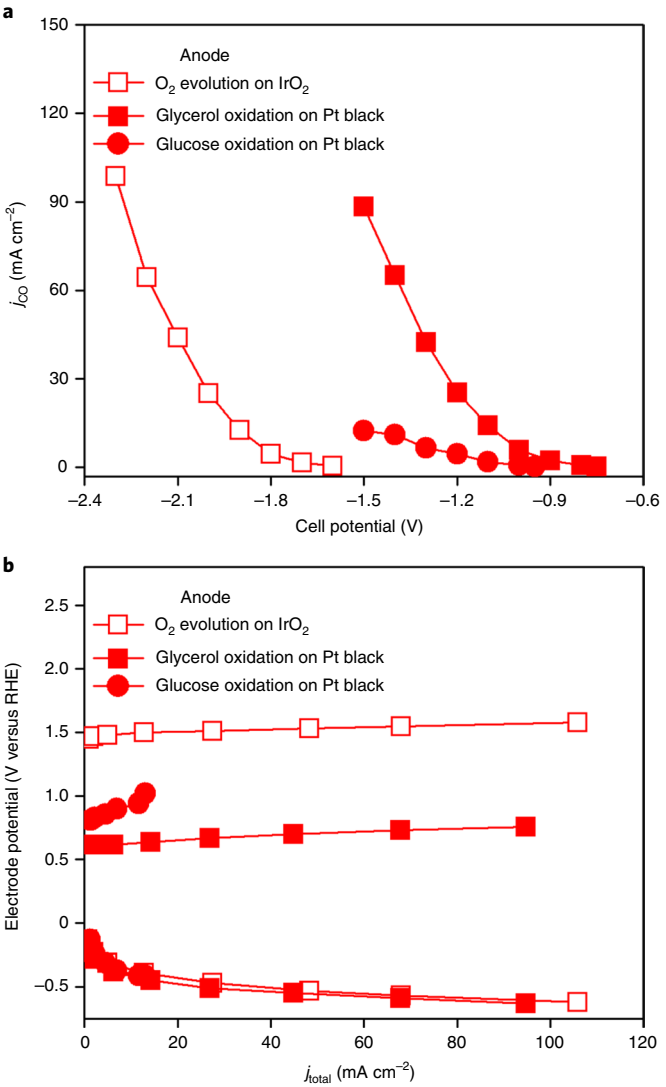

Fig. 4 | Electrochemical performance for the electroreduction of CO_2 to CO on silver, coupled to O_2 evolution, glycerol electro-oxidation or glucose electro-oxidation at the anode. a, j_{CO} as a function of the cell potential. **b**, Individual electrode potential as a function of j_{total}. The cathode was a 1 ± 0.1 mg cm^{-2} silver nanoparticle-coated GDL electrode. The anode was a 1 ± 0.1 mg cm^{-2} IrO_2-coated GDL electrode for O_2 evolution, and a 1 ± 0.1 mg cm^{-2} platinum black-coated GDL electrode for glycerol and glucose electro-oxidation. The catholyte was 2.0 M KOH. The anolyte was 2.0 M KOH for O_2 evolution, 2.0 M KOH + 2.0 M glycerol for glycerol electro-oxidation, and 2.0 M KOH + 2.0 M glucose for glucose electro-oxidation. All data were collected under ambient conditions of 1 atm and 293 K.

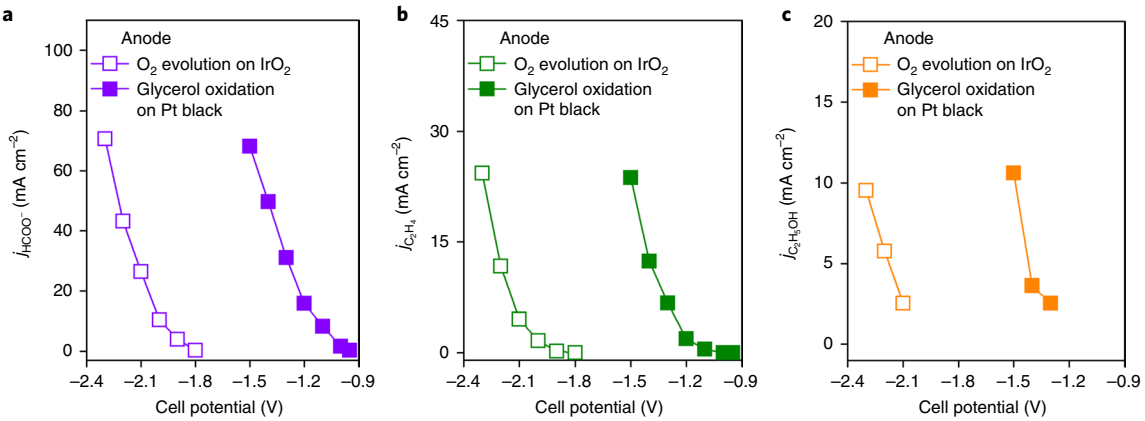

Fig. 5 | Electrochemical performances for the electroreduction of CO_2 to $HCOO^-$ on tin, and to C_2H_4 and C_2H_5OH on copper, coupled to O_2 evolution or glycerol electro-oxidation at the anode. a–c, j_{HCOO^-} (**a**), $j_{C_2H_4}$ (**b**) and $j_{C_2H_5OH}$ (**c**) as a function of the cell potential for the electroreduction of CO_2 on 1 ± 0.1 mg cm^{-2} tin or copper nanoparticle-coated GDL cathodes. The anode was a 1 ± 0.1 mg cm^{-2} IrO_2-coated GDL electrode for O_2 evolution and a 1 ± 0.1 mg cm^{-2} platinum black-coated GDL electrode for glycerol electro-oxidation. The catholyte was 2.0 M KOH. The anolyte was 2.0 M KOH for O_2 evolution, and 2.0 M KOH + 2.0 M glycerol for glycerol electro-oxidation. All data were collected under ambient conditions of 1 atm and 293 K.

product. In special cases of coupling the electroreduction of CO_2 to CH_3OH, C_2H_4 or C_2H_5OH on the cathode with the electro-oxidation of glucose to gluconic acid on the anode, the process becomes spontaneous ($\Delta G^0_{reaction} < 0$); that is, it behaves like a fuel cell and can thus, in principle, be used for the simultaneous production of electricity and carbon chemicals.

The promise of CO_2 and glycerol co-electrolysis

As indicated by the Gibbs free energy analysis, many different anode reactions other than the OER can be utilized to lower $|E^0_{cell}|$, and hence the overall electricity requirements for CO_2 electroreduction. To assess the practicality of such processes, we performed an experimental electroanalytical evaluation of the different combinations proposed in Table 2, using a gas diffusion layer (GDL) electrode-based dual electrolyte channel flow electrolyser under ambient conditions[45,46]. The catholyte was chosen as 2.0 M KOH, which was previously demonstrated by us to lower overpotentials and improve activity for CO_2 electroreduction[46–48]. The anolyte was chosen as a mixture of 2.0 M KOH and 2.0 M glycerol, a mixture of 2.0 M KOH and 2.0 M glucose, and 2.0 M KOH for the electro-oxidation of glycerol, glucose and CH_4, respectively[49].

The electro-oxidation of glycerol or glucose on a platinum black-coated GDL anode coupled to the electroreduction of CO_2 on a silver-coated GDL cathode resulted in significant lowering (that is, a less negative value) of the onset cell potential for CO formation, with values of −0.75 and −0.95 V being observed, respectively, compared with the state-of-the-art value of −1.6 V with the OER at the anode (Fig. 4a). However, the activity (partial current density for CO, j_{CO}) with glucose electro-oxidation ($j_{CO} = 12.47$ mA cm^{-2} or production rate = 0.065 kgCO m^{-2} h^{-1} at a cell potential of −1.5 V) was much lower than with glycerol electro-oxidation ($j_{CO} = 88.44$ mA cm^{-2} or production rate = 0.462 kgCO m^{-2} h^{-1} at a cell potential of −1.5 V) at the anode, limiting the prospects of utilizing glucose as the anode feed. The experimental onset cell potential of −0.75 V for CO production, when using the anodic glycerol electro-oxidation, also fulfils the $V_{max\ (CO_2\ emission)}$ criteria for several process conditions listed in Table 1 that were originally unsatisfied by the −1.6 V value with the OER at the anode. These results indicate that the electroreduction of CO_2 to CO could indeed become carbon neutral and/or negative from the cradle to the gate, even when using the present-day grid electricity mix to drive the process. Depending on the j_{CO} value, the electro-oxidation of glycerol at the anode instead of the OER results in a 37–53% reduction in electricity requirements, thus improving the process economics. A single-electrode plot suggests the major improvement to be at the anode, with the cathodic CO_2 electroreduction remaining unaffected (Fig. 4b). Anodic glycerol electro-oxidation results in the formation of value-added chemicals such as $HCOO^-$ and lactate, which further improve the economics of the overall process (Supplementary Fig. 2). Furthermore, we also evaluated the durability of CO_2–glycerol co-electrolysis with respect to CO production (Supplementary Fig. 3). The results indicate that the cell potential and Faradaic efficiency for CO were stable over a 1.5 h time period. However, flooding of the electrolyte through the cathode GDL was observed at ~1.5 h (similar to earlier observations in the literature)[48], indicating the need to develop more durable GDLs to improve the prospects of this process.

A similar lowering in onset cell potentials for the electroreduction of CO_2 to $HCOO^-$, C_2H_4 and C_2H_5OH was observed when utilizing the electro-oxidation of glycerol at the anode instead of the OER (Fig. 5a). For example, the onset cell potentials for the electroreduction of CO_2 to $HCOO^-$ on a tin-coated GDL cathode, and to C_2H_4 and C_2H_5OH on a copper-coated GDL cathode were −0.9, −0.95 and −1.3 V, respectively, with the anodic electro-oxidation of glycerol, compared with −1.75, −1.8 and −2.1 V with the anodic OER (Fig. 5b,c). Although, the lower-onset cell potentials for C_2H_4 and C_2H_5OH production still do not satisfy the $V_{max\ (CO_2\ emission)}$ criteria, they improve the process economics by satisfying, or getting closer to, the $V_{max\ (gross\ margin)}$ criteria at realistic electricity prices of US$0.04 and US$0.06 kWh^{-1}. On a side note, preliminary experiments on the electro-oxidation of CH_4 on platinum black-, copper-, palladium-, IrO_2- or Pt–Ru black-coated GDL anodes coupled to the electroreduction of CO_2 on a silver-coated GDL cathode did not result in a change in the onset cell potentials for CO production, compared with the OER at the anode. Of course, this is expected due to the high dissociation enthalpy of the C–H bond in CH_4 (435 kJ mol^{-1})[50].

Conclusions

In summary, we have shown that the prospects of CO_2 electroreduction, in terms of both cradle-to-gate CO_2 emissions and economics, can be drastically improved by looking beyond the conventionally used OER at the anode, which essentially acts as an energy sink. Our findings indicate that several different anodic reactions are available to replace the OER, thereby yielding superior thermodynamic

processes with a lower $|E^0_{cell}|$ value. Of the alternatives, the electro-oxidation of glycerol (a cheap industrial waste) seems particularly promising, with the resulting process (co-electrolysis of CO_2 and glycerol) lowering the electricity requirements for conventional CO_2 electroreduction approaches by up to 53%. This alternative process offers avenues for integrating two different CO_2 utilization/mitigation approaches (that is, CO_2 electroreduction and biodiesel production). Furthermore, with the future development of more active and selective catalysts (particularly for glycerol electro-oxidation), co-electrolysis of CO_2 and glycerol can be improved even further, resulting in low-energy pathways for the production of carbon chemicals from waste CO_2. However, it is important to note that the global production of glycerol in 2014 was ~2 Mt yr^{-1} and is projected to grow to only 6 Mt yr^{-1} by 2025[42]. This is several orders of magnitude smaller than the scale of excess global CO_2 emissions (that is, 4 GtC yr^{-1} or 14.7 $GtCO_2$ yr^{-1}). Hence, even in the best case of utilizing carbon-free renewables to drive the co-electrolysis of CO_2 and glycerol to produce CO and/or HCOOH (that is, every mole of glycerol consumes ~4 moles of CO_2, as shown in Table 2 and Supplementary Table 4), the CO_2 emissions that could be addressed would be less than 0.1% of the excess CO_2 emissions. However, a drastic increase in the penetration of biodiesel (a key source of excess glycerol) into the transportation sector would improve the projected impact of the co-electrolysis of CO_2 and glycerol, although, ultimately, it will be limited by the scale of the overall carbon chemicals market. Another interesting process to further investigate would be the co-electrolysis of CO_2 and CH_4. In addition to the attractive prospects of reducing the electricity consumption and hence the cradle-to-gate CO_2 emissions, co-electrolysis of CO_2 and CH_4 could circumvent the issues of scale associated with the co-electrolysis of CO_2 and glycerol. Significant research into the development of electrocatalysts and electrochemical systems for the co-electrolysis of CO_2 and CH_4 would be needed to make the process practical.

Methods

General. Unless stated otherwise, all experiments were performed under ambient conditions of 1 atm and 293 K, all commercially available materials were used as received, and >18.0 MΩ cm deionized water was used when required.

Preparation of catalyst-coated GDL electrodes. Commercially available silver (<100 nm; Sigma–Aldrich; product number: 576832), tin (<150 nm; Sigma–Aldrich; product number: 576883) and copper (40–60 nm; Sigma–Aldrich; product number: 774111) nanoparticles were used as the cathode catalysts to study the electroreduction of CO_2 to CO, $HCOO^-$, and C_2H_4 and C_2H_5OH, respectively. The nanoparticles were first made into an ink by sonicating 20 mg of the material (silver or tin) with 800 µl of deionized water (800 µl tetrahydrofuran was used instead of deionized water for copper), 52 µl of Nafion solution (5 wt.%; Fuel Cell Earth) and 800 µl of isopropyl alcohol, for 20 min. The resulting catalyst ink was then deposited onto a Sigracet 35 BC GDL with a geometric surface area of 5 × 2 cm^2 (corresponding to 4 electrodes) using an automated airbrush method[51], to form the catalyst-coated gas diffusion cathodes. Nearly 50% of the starting catalyst material was lost during the automated airbrush deposition process, resulting in a final catalyst loading of 1 ± 0.1 mg cm^{-2}, which was estimated by weighing the cathodes before and after the deposition process. The OER at the anode was studied using IrO_2 non-hydrate (Alfa Aesar; product number: 43396). The electro-oxidation of glycerol and glucose at the anode was studied using platinum black high surface area (Alfa Aesar; product number: 43838). The electro-oxidation of CH_4 was studied using IrO_2 non-hydrate platinum black, copper or palladium (0.25–0.55 µm; Alfa Aesar; product number: 00776) and Pt–Ru black (Alfa Aesar; product number: 41171) as the anode catalyst. The catalyst-coated GDL anodes were prepared according to a process very similar to the one described for making the cathodes. That is, 20 mg of the catalyst material was sonicated with 800 µl of deionized water, 52 µl of Nafion solution and 800 µl of isopropyl alcohol for 20 min to make a catalyst ink, followed by the deposition of the ink onto a Sigracet 35 BC GDL (geometric area = 5 × 2 cm^2, corresponding to 4 electrodes) via an automated airbrush method. All catalyst-coated GDL anodes had a final loading of 1 ± 0.1 mg cm^{-2}, as estimated by weighing the anodes before and after the deposition process.

Preparation of electrolytes. The electrolytes used in this work were prepared by dissolving the appropriate amount of the salt and/or chemical in deionized water. The salts and chemicals used were: potassium hydroxide (Fisher Chemical; product number: P250); glycerol (Alfa Aesar; product number: 38988); and D-(+)-glucose (Sigma Life Science; product number: 49139). The pH and conductivity of the different electrolytes were measured using an Orion 4-star pH conductivity meter.

Electroanalysis in a flow electrolyser. The electrochemical characterization of the different combinations of CO_2 electroreduction at the cathode with the O_2 evolution reaction and glycerol, glucose or CH_4 electro-oxidation at the anode was performed in a gas diffusion electrode-based dual electrolyte channel flow electrolyser with a precisely machined active geometric area of 1 cm^2, as described previously by us[45,46]. The catholyte and anolyte chamber were separated by a Fumapem FAA-3-PK-75 anion exchange membrane to prevent crossover of the liquid products from the cathode to the anode and vice versa. The catholyte for all experiments was 2.0 M KOH. The anolyte for studying the OER and CH_4 electro-oxidation was 2.0 M KOH, whereas the anolytes for studying the electro-oxidation of glycerol and glucose were 2.0 M KOH + 2.0 M glycerol and 2.0 M KOH + 2.0 M glucose, respectively. Electrochemical experiments were performed by maintaining a constant cell potential using a potentiostat (Autolab PGSTAT30; Eco Chemie). The individual cathode and anode potentials were measured with a multimeter (AMPROBE 15XP-B) connected between the appropriate electrode and an Ag/AgCl reference electrode (3 mol kg^{-1}; RE-5B BASi). The individual electrode potentials (versus Ag/AgCl) were then converted to the reversible hydrogen electrode (RHE) scale using the Nernst equation: $E_{RHE} = E_{Ag/AgCl} + 0.210 + 0.058 \times pH$. All cell, cathode and anode potentials in this study are reported as measured, without any current and resistance (*iR*) corrections. The CO_2 (Airgas) feed for the reaction was provided as a continuous stream over the teflonized side of the cathode GDL using a flow controller (Smart-Trak 2; Sierra Instruments). A CO_2 flow rate of 17 standard cubic centimetres per minute (sccm) was maintained for cell potentials at which the total current density (j_{total}) was >5 mA cm^{-2}, and lowered to 5 sccm for cell potentials at which j_{total} was <5 mA cm^{-2}, to enable a gas product analysis with high sensitivity. A pressure controller (Cole Parmer; 00268TC) was used in the electrolyser downstream to maintain a low pressure of 14.20 psi and thus facilitate an easy transfer of the gas products from the cathode GDL to the effluent gas stream. A low downstream pressure also minimizes the dissolution of the reacting CO_2 and gas products into the electrolyte stream. Both the catholyte and the anolyte stream were circulated through the electrolyte channels of the electrolyser using a syringe pump (PHD 2000; Harvard Apparatus) at flow rate of 0.5 ml min^{-1} for cell potentials at which j_{total} was >5 mA cm^{-2}, and lowered to 0.2 ml min^{-1} for cell potentials at which j_{total} was <5 mA cm^{-2}, to enable a liquid product analysis with high sensitivity. For all electrochemical experiments, after a particular cell potential was switched on, the resulting current was allowed to stabilize for at least 180 s before the product analysis was initiated.

Product analysis. For a particular cell potential, the gas products of CO_2 electroreduction were analysed for a total time period of 180 s by diverting 1 ml of the effluent gas stream three times, at regular intervals of 90 s, to an on-line gas chromatograph (a Thermo Finnigan Trace GC with a Carboxen 1000 column from Supelco). The gas chromatograph was equipped with both the thermal conductivity detector and the flame ionization detector. Helium with a flow rate of 20 sccm was used as the carrier gas. The concentration of the gas products was quantified by averaging the peak areas over the three sample injections and using the appropriate calibration curves. Meanwhile, the liquid products were analysed for the same 180 s time period by collecting both the catholyte and the anolyte streams followed by ex situ ^{1}H NMR (UI500NB; Varian) analysis (16 scans with solvent suppression). The liquid samples for the ^{1}H NMR analysis were prepared by mixing 100 µl of the collected electrolyte with 400 µl of D_2O (Sigma–Aldrich; product number: 151882) and 100 µl of an internal standard comprising 1.25 mM dimethyl sulfoxide in D_2O. The concentration of the liquid products was quantified using the appropriate calibration curves. The total current density (that is, the total current, as the electrolyser area was 1 cm^2) was quantified by averaging the data obtained during the same 180 s time period when the CO_2 electroreduction products were being analysed. The Faradaic efficiency for the different CO_2 electroreduction products was calculated per the following equation:

$$\mathrm{FE}(\%) = \frac{znF}{Q} \times 100$$

where n is the number of moles of the product formed and Q is the amount of charge passed. The partial current density for a particular product was calculated by multiplying j_{total} by the Faradaic efficiency for that product. The onset cell potential for a specific CO_2 electroreduction product defined in this work refers to the lowest (least negative) cell potential at which the product was first observed in the gas chromatograph (for gas products) or ^{1}H NMR analysis (for liquid products).

Data availability

The electrochemical data that support the plots, as well other findings of this study, are available in the Supplementary Information.

Received: 9 January 2018; Accepted: 18 March 2019;
Published online: 22 April 2019

References

1. IPCC *Climate Change 2013: The Physical Science Basis* (eds Stocker, T. F. et al.) (Cambridge Univ. Press, 2013).
2. *Adoption of the Paris Agreement* FCCC/CP/2015/L.9/Rev.1 (UNFCCC, 2015).
3. Pacala, S. & Socolow, R. Stabilization wedges: solving the climate problem for the next 50 years with current technologies. *Science* **305**, 968–972 (2004).
4. Chu, S. & Majumdar, A. Opportunities and challenges for a sustainable energy future. *Nature* **488**, 294–303 (2012).
5. Leung, D. Y. C., Caramanna, G. & Maroto-Valer, M. M. An overview of current status of carbon dioxide capture and storage technologies. *Renew. Sustain. Energy Rev.* **39**, 426–443 (2014).
6. Herron, J. A., Kim, J., Upadhye, A. A., Huber, G. W. & Maravelias, C. T. A general framework for the assessment of solar fuel technologies. *Energy Environ. Sci.* **8**, 126–157 (2015).
7. Jhong, H. R. M., Ma, S. & Kenis, P. J. A. Electrochemical conversion of CO_2 to useful chemicals: current status, remaining challenges, and future opportunities. *Curr. Opin. Chem. Eng.* **2**, 191–199 (2013).
8. Hietala, J. et al. in *Ullmann's Encyclopedia of Industrial Chemistry* 1–22 (Wiley-VCH, 2016).
9. Bierhals, J. in *Ullmann's Encyclopedia of Industrial Chemistry* 679–693 (Wiley-VCH, 2001).
10. Hammer, G. et al. in *Ullmann's Encyclopedia of Industrial Chemistry* 739–792 (Wiley-VCH, 2006).
11. Ott, J. et al. in *Ullmann's Encyclopedia of Industrial Chemistry* 1–27 (Wiley–VCH, 2012).
12. Zimmermann, H. & Walzl, R. in *Ullmann's Encyclopedia of Industrial Chemistry* 465–529 (Wiley-VCH, 2009).
13. Kosaric, N. et al. in *Ullmann's Encyclopedia of Industrial Chemistry* 333–403 (Wiley-VCH, 2011).
14. Hori, Y., Wakebe, H., Tsukamoto, T. & Koga, O. Electrocatalytic process of CO selectivity in electrochemical reduction of CO_2 at metal electrodes in aqueous media. *Electrochim. Acta* **39**, 1833–1839 (1994).
15. Hori, Y. in *Modern Aspects of Electrochemistry* 89–189 (Springer, 2008).
16. Qiao, J. L., Liu, Y. Y., Hong, F. & Zhang, J. J. A review of catalysts for the electroreduction of carbon dioxide to produce low-carbon fuels. *Chem. Soc. Rev.* **43**, 631–675 (2014).
17. Kumar, B. et al. New trends in the development of heterogeneous catalysts for electrochemical CO_2 reduction. *Catal. Today* **270**, 19–30 (2016).
18. Lu, Q. & Jiao, F. Electrochemical CO_2 reduction: electrocatalyst, reaction mechanism, and process engineering. *Nano Energy* **29**, 439–456 (2016).
19. Khezri, B., Fisher, A. C. & Pumera, M. CO_2 reduction: the quest for electrocatalytic materials. *J. Mater. Chem. A* **5**, 8230–8246 (2017).
20. Sharma, P. P. & Zhou, X. D. Electrocatalytic conversion of carbon dioxide to fuels: a review on the interaction between CO_2 and the liquid electrolyte. *WIREs Energy Environ.* **6**, e239 (2017).
21. Endrődi, B. et al. Continuous-flow electroreduction of carbon dioxide. *Prog. Energy Combust. Sci.* **62**, 133–154 (2017).
22. Verma, S., Kim, B., Jhong, H. R. M., Ma, S. & Kenis, P. J. A. A gross-margin model for defining technoeconomic benchmarks in the electroreduction of CO_2. *ChemSusChem* **9**, 1972–1979 (2016).
23. Li, X. P. et al. Greenhouse gas emissions, energy efficiency, and cost of synthetic fuel production using electrochemical CO_2 conversion and the Fischer–Tropsch process. *Energy Fuels* **30**, 5980–5989 (2016).
24. *eGRID2014 v2* (US Environmental Protection Agency, 2017).
25. *Annual Energy Outlook* (US Energy Information Administration, 2017).
26. Yazdani, S. S. & Gonzalez, R. Anaerobic fermentation of glycerol: a path to economic viability for the biofuels industry. *Curr. Opin. Biotechnol.* **18**, 213–219 (2007).
27. Simoes, M., Baranton, S. & Coutanceau, C. Electrochemical valorisation of glycerol. *ChemSusChem* **5**, 2106–2124 (2012).
28. David, J. & Herzog, H. The cost of carbon capture. In *5th International Conference on Greenhouse Gas Control Technologies (GHGT-5)* 985–990 (CSIRO, 2001).
29. Bains, P., Psarras, P. & Wilcox, J. CO_2 capture from the industry sector. *Prog. Energy Combust. Sci.* **63**, 146–172 (2017).
30. *Inventory of U.S. Greenhous Gas Emissions and Sinks (1990–2015)* (US Environmental Protection Agency, 2017).
31. Kuramochi, T., Ramîrez, A., Turkenburg, W. & Faaij, A. Comparative assessment of CO_2 capture technologies for carbon-intensive industrial processes. *Prog. Energy Combust. Sci.* **38**, 87–112 (2012).
32. Kim, B., Ma, S., Jhong, H. R. M. & Kenis, P. J. A. Influence of dilute feed and pH on electrochemical reduction of CO_2 to CO on Ag in a continuous flow electrolyzer. *Electrochim. Acta* **166**, 271–276 (2015).
33. House, K. Z. et al. Economic and energetic analysis of capturing CO_2 from ambient air. *Proc. Natl Acad. Sci. USA* **108**, 20428–20433 (2011).
34. Sherman, S. R. et al. Compilation and correlation of limiting activity coefficients of nonelectrolytes in water. *Ind. Eng. Chem. Res.* **35**, 1044–1058 (1996).
35. Robinson, R. A. & Stokes, R. H. Tables of osmotic and activity coefficients of electrolytes in aqueous solution at 25 °C. *Trans. Faraday Soc.* **45**, 612–624 (1949).
36. Cussler, E. L. & Dutta, B. K. On separation efficiency. *AIChE J.* **58**, 3825–3831 (2012).
37. Kiss, A. A., Landaeta, S. J. F. & Ferreira, C. A. I. Towards energy efficient distillation technologies—making the right choice. *Energy* **47**, 531–542 (2012).
38. Mudd, G. M. Sustainability reporting and the platinum group metals: a global mining industry leader? *Platin. Met. Rev.* **56**, 2–19 (2012).
39. Bard, A. J., Parsons, R. & Jordan, J. *Standard Potentials in Aqueous Solutions* (CRC Press, 1985).
40. Bevilacqua, M. et al. Energy savings in the conversion of CO_2 to fuels using an electrolytic device. *Energy Technol.* **2**, 522–525 (2014).
41. Li, T. F., Cao, Y., He, J. F. & Berlinguette, C. P. Electrolytic CO_2 reduction in tandem with oxidative organic chemistry. *ACS Cent. Sci.* **3**, 778–783 (2017).
42. Ciriminna, R., Della Pina, C., Rossi, M. & Pagliaro, M. Understanding the glycerol market. *Eur. J. Lipid Sci. Technol.* **116**, 1432–1439 (2014).
43. Malakoff, D. The gas surge. *Science* **344**, 1464–1467 (2014).
44. Von der Assen, N., Jung, J. & Bardow, A. Life-cycle assessment of carbon dioxide capture and utilization: avoiding the pitfalls. *Energy Environ. Sci.* **6**, 2721–2734 (2013).
45. Whipple, D. T., Finke, E. C. & Kenis, P. J. A. Microfluidic reactor for the electrochemical reduction of carbon dioxide: the effect of pH. *Electrochem. Solid State Lett.* **13**, D109–D111 (2010).
46. Ma, S. et al. One-step electrosynthesis of ethylene and ethanol from CO_2 in an alkaline electrolyzer. *J. Power Sources* **301**, 219–228 (2016).
47. Verma, S., Lu, X., Ma, S., Masel, R. I. & Kenis, P. J. A. The effect of electrolyte composition on the electroreduction of CO_2 to CO on Ag based gas diffusion electrodes. *Phys. Chem. Chem. Phys.* **18**, 7075–7084 (2016).
48. Verma, S. et al. Insights into the low overpotential electroreduction of CO_2 to CO on a supported gold catalyst in an alkaline flow electrolyzer. *ACS Energy Lett.* **3**, 193–198 (2018).
49. Kwon, Y., Lai, S. C. S., Rodriguez, P. & Koper, M. T. M. Electrocatalytic oxidation of alcohols on gold in alkaline media: base or gold catalysis? *J. Am. Chem. Soc.* **133**, 6914–6917 (2011).
50. Narsimhan, K., Iyoki, K., Dinh, K. & Roman-Leshkov, Y. Catalytic oxidation of methane into methanol over copper-exchanged zeolites with oxygen at low temperature. *ACS Cent. Sci.* **2**, 424–429 (2016).
51. Jhong, H. R., Brushett, F. R. & Kenis, P. J. A. The effects of catalyst layer deposition methodology on electrode performance. *Adv. Energy Mater.* **3**, 589–599 (2013).

Acknowledgements

The authors acknowledge financial support from the International Institute for Carbon Neutral Energy Research (WPI-I2CNER), sponsored by the Japanese Ministry of Education, Culture, Sports, Science and Technology, as well as the Dow Chemical Company, and Glenn E. and Barbara R. Ullyot for graduate fellowships to S.V. The ^{1}H NMR experiments were performed in the School of Chemical Sciences NMR Laboratory at the University of Illinois.

Author contributions

S.V. conceived the project, performed the cradle-to-gate CO_2 analysis, designed and conducted the electrochemical experiments, analysed the data and wrote the manuscript. S.L. prepared the electrodes, contributed to the electrochemical experiments and commented on the manuscript. P.J.A.K. conceived the project, directed the research and wrote the manuscript.

Competing interests

The authors have filed a patent application (US patent application number 15/971,223) on technology related to the processes described in this article.

Additional information

Supplementary information is available for this paper at https://doi.org/10.1038/s41560-019-0374-6.

Reprints and permissions information is available at www.nature.com/reprints.

Correspondence and requests for materials should be addressed to P.J.A.K.

Publisher's note: Springer Nature remains neutral with regard to jurisdictional claims in published maps and institutional affiliations.